

Influenza Virus Polymerase Basic Protein 1 Interacts with Influenza Virus Polymerase Basic Protein 2 at Multiple Sites

SIDDHARTHA K. BISWAS AND DEBI P. NAYAK*

Department of Microbiology and Immunology and Jonsson Comprehensive Cancer Center, UCLA School of Medicine, Los Angeles, California 90024-1747

Received 22 April 1996/Accepted 24 June 1996

Three polymerase proteins of influenza type A virus interact with each other to form the active polymerase complex. Polymerase basic protein 1 (PB1) can interact with PB2 in the presence or absence of polymerase acidic protein. In this study, we investigated the domains of PB1 involved in complex formation with PB2 in vivo, using coexpression and coimmunoprecipitation of the PB1-PB2 complex with monospecific antibodies. Results show that PB1 possesses at least two regions which can interact independently and form stable complexes with PB2. Both of these regions are located at the NH₂ terminus of PB1; the COOH-terminal half of PB1 is not involved in interacting with PB2. Deletion analysis further demonstrated that the interacting regions of PB1 encompass amino acids (aa) 48 to 145 and aa 251 to 321. Linker insertions throughout the PB1 sequences did not affect complex formation with PB2. Deletion and linker-insertion mutants of PB1 were tested for polymerase activity in vivo. For this analysis, we developed a simplified assay for viral polymerase activity that uses a reporter chloramphenicol acetyltransferase gene containing the 5' and 3' ends of influenza viral promoter and nontranslating regions (minus sense) of the NS gene joined to a hepatitis delta virus ribozyme at its 3' end. This assay demonstrated that all deletion mutants of PB1 exhibited either background or greatly reduced polymerase activity irrespective of the ability to interact with PB2 and that all linker-insertion mutants except one at the extreme COOH end (L-746) of PB1 were also negative for viral polymerase activity. These results show that compared with complex formation of PB1 with PB2, the polymerase activity of PB1 was extremely sensitive to structural perturbation.

Influenza viruses, which are segmented negative-strand RNA viruses, carry an RNA-dependent RNA polymerase known as transcriptase/replicase. Transcription and replication of viral RNA occur in the cell nucleus by the viral ribonucleoprotein (RNP)-polymerase complex, which consists of at least three polymerase (P) proteins and NP and viral RNA as the template. Three polymerase proteins are known to function as a heterocomplex. They are found to be tightly associated with the double-stranded panhandle formed by the 5' and 3' termini of each viral RNA segment (8, 14, 17). Studies have also shown that three polymerase proteins can exist as 3P heterocomplex free from viral RNP in virus-infected cells (2, 7) as well as in cells expressing polymerase proteins (4, 15, 16), indicating that three P proteins interact with each other in the absence of other viral proteins. However, such interaction among the three polymerase proteins may be dynamic in nature and may vary depending on the mode of transcription or replication of viral RNA. Recently, it was shown that cooperation and possibly complex formation of three proteins are required for cap recognition and cap cleavage of host mRNA by PB2 (5, 11, 35) and for cap-dependent transcription of viral mRNA, but the function of polymerase basic protein 2 (PB2) may not be essential for cap-independent replication (22). Thus, the cooperative functions of different polymerase proteins and the presence of 3P heterocomplex in both virus-infected and coexpressing cells suggest that the interactions among the polymerase proteins are critical for viral transcription and replication. We and others have initiated studies to elucidate the functional domains of polymerase proteins, including localization of nuclear targeting signals (21, 23, 25), catalytic activity of PB1 (4), and interacting domains among the polymerase proteins (28). Recently, Perez

and Donis (28) have shown that the NH₂ terminus of PB1 interacts with polymerase acidic protein (PA). Nakagawa et al. (22) have demonstrated that PB1 and PB2 function cooperatively in cap-dependent mRNA transcription, as PB2 provides the cap recognition and cap cleavage activity and PB1 provides the polymerizing activity leading to RNA chain elongation. Furthermore, PB1 and PB2 can interact with each other and form a stable complex in the absence of viral RNA, viral RNP, or other viral proteins in insect cells in assays using the baculovirus expression system (34) as well as in mammalian cells (4). In this study, we investigated the domains of PB1 interacting with PB2 and found that at least two sites of PB1 can interact with PB2 independently.

To define the functions of individual polymerase proteins, a reconstitution system in which individual components of transcription and replication can be added to constitute a functional polymerase complex is essential. However, such a system suitable for reconstituting the functional polymerase complex for transcription and replication in vitro is not available. To circumvent this problem, we (4) and others (6, 18–20, 24) have used an in vivo reconstitution system which consists of the expression of individual polymerase proteins in eukaryotic cells. Using this in vivo reconstitution system, one can analyze the requirements of individual polymerase proteins by using the transcription and replication of a reporter gene containing the promoter elements of influenza virus RNA. However, in this system, the reporter gene is introduced into cells as RNP (18), which is labor-intensive as it requires the reconstitution of viral RNP containing viral RNA, NP, and polymerase proteins isolated from purified viruses. Although another group (7) has successfully used naked viral RNA in transfection, this approach is rather inefficient and not widely used. In this study, we modified this system by using a hepatitis delta virus ribozyme and T7 polymerase so that the reporter gene is intro-

* Corresponding author.

duced as cDNA and the RNA transcribed inside the cell is converted into viral RNP with precise 5' and 3' ends (3). Using this transcription-replication system, we have analyzed deletion and linker-insertion mutants of PB1 for transcription and replication of viral RNA and found that the transcription-replication function of PB1 is highly sensitive to structural perturbation.

MATERIALS AND METHODS

Viruses and cells. A/WSN/33 (H1N1) virus was grown in MDCK cells (4). Recombinant vaccinia virus expressing T7 RNA polymerase (VTF7.3) was obtained from Bernard Moss, National Institute of Allergy and Infectious Diseases, Bethesda, Md. (10). Stocks of recombinant vaccinia viruses were grown in HeLa cells, and infectivity titers were determined in CV1 cells. BHK-21 cells were used to study polymerase protein interactions. COS1 cells were grown in Dulbecco modified Eagle's medium containing 10% fetal bovine serum and used for influenza virus polymerase activity assays.

Plasmids and mutagenesis of the PB1 gene. Plasmids pGEM PB1, pGEM PB2, pGEM PA, and pGEM NP were constructed as described before (4). Except when indicated otherwise, standard techniques were used for DNA manipulation and transformation (31). In-frame deletion mutants were constructed by using restriction enzyme sites to remove DNAs encoding different amino acids from the full-length 757-amino-acid (aa) PB1 protein as follows: del 1 (*EcoRI*), deletion of aa 493 to 757; del 2 (*PstI*), deletion of aa 371 to 757; del 3 (*BclI*), deletion of aa 321 to 757; del 4 (*AccI*), deletion of aa 254 to 757; del 5 (*NcoI* to *AflII*), deletion of aa 34 to 166; del 6 (*AflII* to *AccI*), deletion of aa 169 to 252; del 7 (*AccI* to *BclI*), deletion of aa 254 to 320; del 8 (*NcoI* to *AccI*), deletion of aa 34 to 252; del 9 (*NcoI* to *BalI*), deletion of aa 34 to 320; del 10 (*BalI* to *BalI*), deletion of aa 144 to 320; and del 11 (*BalI* to *XmnI*), deletion of aa 144 to 458. Del 12 to del 18 were constructed by combining the two different in-frame deletion mutants. In brief, the deletions of aa 34 to 144 in del 13, aa 49 to 166 in del 14, aa 49-144 in del 15, aa 49 to 71 in del 16, and aa 71 to 144 in del 18 were constructed by using restriction sites *NcoI* to *BalI*, *ScaI* to *AflII*, *ScaI* to *BalI*, *ScaI* to *Sau96I*, and *Sau96I* to *BalI*, respectively. Using the restriction enzyme *BamHI*, we deleted 90 aa from the C-terminal end of del 16 to construct del 17. Similarly, del 19 to del 24 were constructed by using two different restriction enzyme sites as follows: del 19 (*HindIII* to *NcoI*), deletion of aa 1 to 39; del 20 (*NcoI* to *Sau96I*), deletion of aa 34 to 70; del 21 (*HaeIII* to *AluI*), deletion of aa 71 to 121, del 22 (*ScaI* to *BalI*), deletion of aa 49 to 144; del 23 (*BalI* to *DpnI*), deletion of aa 143 to 181; and del 24 (*AflII* to *AccI*), deletion of aa 169 to 252.

To construct the linker-insertion mutations, the pGEM PB1 DNA was partially cleaved with one of a selected set of restriction enzymes (*HincII*, *AflII*, *AccI*, *XmnI*, *EcoRI*, *PvuII*, or *BglII*), and the linear molecules resulting from a single cut were purified by agarose gel electrophoresis. When necessary, the ends were blunt ended by treatment with the Klenow fragment of DNA polymerase I, and oligonucleotide linkers containing an *XhoI* (New England Biolabs, Beverly, Mass.) cleavage site were ligated to the termini. The DNA was cleaved with *XhoI*, recircularized with T4 DNA ligase, and transformed. DNA was isolated from various clones screened for the presence of the *XhoI* site, and the position of each insertion was determined by restriction mapping and nucleotide sequencing.

Plasmid pIVACAT1, which directs an NS-like transcript containing the chloramphenicol acetyltransferase (CAT) gene (18), was provided by P. Palese, Mount Sinai School of Medicine, New York, N.Y. The transcription vector 2.0, containing hepatitis delta virus ribozyme and T7 termination sequence, was a gift from L. Andrew Ball, University of Alabama, Birmingham (3). Plasmid Ribo-CAT, used in this study to assay influenza virus transcriptase/replicase activity, was constructed as follows: a 680-bp *HindIII*-blunt-ended *HgaI* restriction fragment of pIVACAT1 and a 250-bp *SmaI*-*PstI* restriction fragment from transcription vector 2.0 were ligated to *HindIII*-*PstI* I-digested pUC19 by three-way ligation.

Infection and transfection. For polymerase binding assay, BHK-21 cells in 35-mm-diameter dishes were infected with VTF7.3 at a multiplicity of infection (MOI) of 5 to 10 for 1 h. Unadsorbed viruses were removed by washing with phosphate-buffered saline containing 0.01% CaCl_2 and 0.01% MgCl_2 (PBS^+), and vaccinia virus-infected cells were transfected with a mixture of pGEM PB1 and pGEM PB2 DNAs by Lipofectin (Gibco BRL, Gaithersburg, Md.)-mediated transfection as described previously (4). Cells were incubated for 16 h and then labeled for immunoprecipitation.

For the transcription-replication assay, COS1 cells in 60-mm-diameter dishes were infected with VTF7.3 at an MOI of 5 to 10 for 1 h, washed with PBS^+ , and then transfected with a mixture of plasmids encoding PB1, PB2, PA, and NP (4). In brief, 2 μg each of plasmids pGEM PB1 (or mutant) and pGEM PB2, 0.5 μg of pGEM PA, 5 μg of pGEM NP, and 3 μg of Ribo-CAT DNA were transfected by Lipofectin-mediated transfection. The total amount of transfected DNA per dish was kept constant by adjusting the amount, if necessary, with pGEM3 DNA to avoid differences in transfection efficiency. Twenty-four hours posttransfection (hpt), transfected cells were washed twice with PBS and once with TNE (100 mM NaCl, 50 mM Tris-HCl [pH 7.5], 1 mM EDTA) and lysed by freezing and

thawing (4) in 0.25 M Tris HCl (pH 8.0). The cell lysate was divided into two portions, one processed for Western blotting (immunoblotting) and the other processed for the CAT assay (4).

Radiolabeling, immunoprecipitation, and Western blotting of the polymerase complex. For radiolabeling of proteins, cells at 16 h hpt were washed in PBS^+ , incubated in methionine-free medium for 1 h at 37°C, and labeled for 1 h in 1 ml of methionine-free medium containing 50 μCi of Trans ^{35}S -label (ICN Biochemicals Inc., Irvine, Calif.) per ml. At the end of the labeling, the cell monolayer was washed twice in cold PBS , scraped in cold PBS , and pelleted by centrifugation. For immunoprecipitation of the polymerase complex, the cell pellet was resuspended in radioimmunoprecipitation assay buffer (10 mM Tris-HCl [pH 7.5], 2 mM EDTA, 100 mM NaCl, 1% Nonidet P-40, 0.5% sodium deoxycholate, 0.1% sodium dodecyl sulfate [SDS], 1% aprotinin) and divided into two parts. Each part was immunoprecipitated with a monospecific anti-PB1 or anti-PB2 antibody as described previously (4). Immunoprecipitates were further washed successively with radioimmunoprecipitation assay buffer containing 0.5 and 1 M NaCl. The polymerase complex was analyzed by SDS-polyacrylamide (10%) gel electrophoresis (SDS-PAGE). To determine if the expression levels of the wild-type (WT) and mutant proteins were similar, cell lysates were analyzed by Western immunoblotting. Accordingly, the cell pellet was directly lysed in sample buffer by boiling, and protein samples were subjected to SDS-PAGE and transferred to a Nytran membrane (Schleicher & Schuell, Inc., Keene, N.H.). Polymerase proteins were detected by standard procedures with a monospecific rabbit anti-PB1 antibody and alkaline phosphatase-conjugated anti-rabbit immunoglobulin (4).

CAT assays. Cells were lysed and assessed for CAT activity by standard methods as described previously (4). Each assay was done from two independent experiments. For quantification, autoradiograms were quantified by densitometric analysis using an LKB 2222-020 Ultrascan XL Laser Densitometer (Pharmacia-LKB, Uppsala, Sweden).

RESULTS

Effects of PB1 mutations on the formation of a PB1-PB2 complex. PB1 and PB2 when coexpressed from cDNA formed a stable polymerase complex in vivo in the absence of PA, NP, or other viral proteins and can be coimmunoprecipitated by either an anti-PB1 or an anti-PB2 antibody (4). To determine the specific sites in PB1 responsible for interaction with PB2, monolayers of BHK-21 cells were infected with VTF7.3, a recombinant vaccinia virus expressing bacteriophage T7 RNA polymerase (10), for 1 h at 37°C. These VTF7.3-infected cells were then transfected with pGEM PB1 and pGEM PB2 DNA (both PB1 and PB2 cDNAs were under the control of T7 RNA polymerase promoter). At 16 hpt, transfected cells were labeled with Trans ^{35}S -label for 1 h and lysed, and equal amounts of lysates were immunoprecipitated with either a monospecific anti-PB1 antibody or anti-PB2 antibody as described in Materials and Methods. The results show that the WT and mutant proteins were expressed efficiently (Fig. 1, 3, and 4, lanes PB1+PB2). When PB1 or PB2 was expressed alone and immunoprecipitated with the anti-PB2 (Fig. 1B, lane PB1) or anti-PB1 (Fig. 1A, lane PB2) antibody, respectively, each protein was immunoprecipitated only by the homologous antibody, demonstrating the specificity of each antibody. However, when PB1 and PB2 were coexpressed, either the anti-PB1 (Fig. 1A, lane PB1+PB2) or the anti-PB2 (Fig. 1B, lane PB1+PB2) antibody immunoprecipitated both PB1 and PB2 proteins, demonstrating that PB1 and PB2 formed a stable polymerase complex as was also observed in WSN-infected cells (Fig. 1). To locate the regions of PB1 important for interaction with the PB2 protein, a series of PB1 deletion mutants was constructed (Fig. 2). These deletions were made to create a panel of mutants essentially encompassing the entire coding region of PB1 except for the first 33 residues. Initially, four mutant PB1 cDNAs encoding various lengths of COOH-terminal deletion of PB1 protein were constructed by using the restriction enzyme sites within the PB1 cDNA (Fig. 2, del 1 to del 4). These mutant PB1 proteins lacked 265, 387, 437, and 504 aa, respectively from the COOH-terminal end. In addition, in-frame deletion mutants (del 5 to del 18) were constructed by filling the overhang generated by a restriction endonuclease and re-

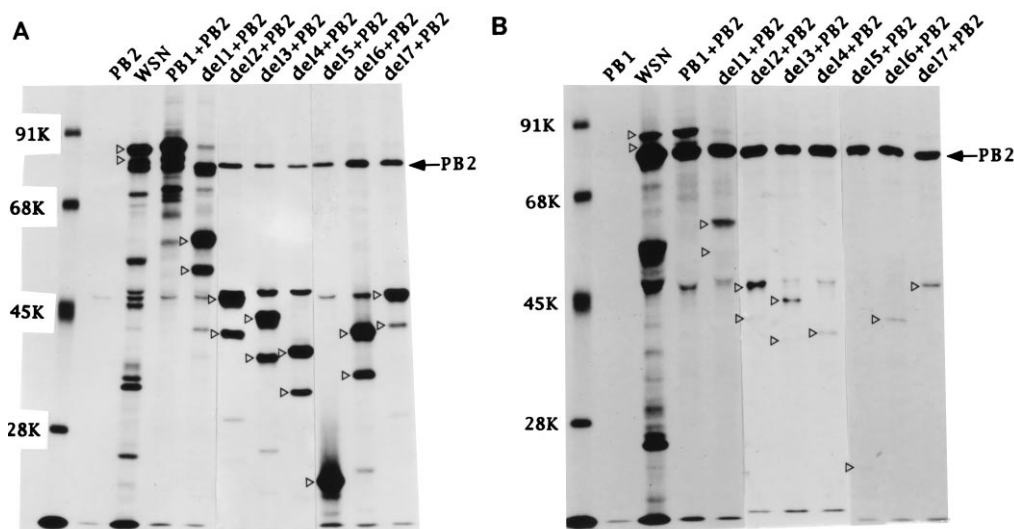


FIG. 1. Coexpression and coimmunoprecipitation of PB1 and PB2. BHK-21 cells were infected with VTF.3 at an MOI of 5 for 1 h and cotransfected with WT PB2 DNA (6 μ g) and either WT or mutant PB1 DNA (del 1 to del 7; 4 μ g). The cells were labeled at 16 hpt with Trans 35 S-label (50 μ Ci/ml) for 1 h and lysed as described in Materials and Methods. The lysate was divided into two aliquots, and each aliquot was immunoprecipitated with a monospecific anti-PB1 (A) or anti-PB2 (B) antibody (2). The immunoprecipitates were analyzed by SDS-PAGE. Positions of PB1 (arrowheads) and PB2 (arrows) are shown.

ligating as described in Materials and Methods. The nature and positions of the in-frame deletion mutants are shown in Fig. 2. In all cases, the sequences of these altered genes retained the PB1 translational reading frame so that the mutant polypeptides could be immunoprecipitated with the anti-PB1 antibody. These deletion mutants were coexpressed with WT

PB2 in the VTF.3 expression system, and the labeled cell lysates were immunoprecipitated with either the anti-PB1 or the anti-PB2 antibody. Results show that when immunoprecipitated with the anti-PB1 antibody, PB1 mutants del 1 to del 7 were detected as distinct polypeptides of the expected sizes (Fig. 1A, lane del 1+PB2 to del 7+PB2). In addition, a faster-migrating PB1 band was found in all lanes. A similar faster-migrating band presumably arising from internal translation initiation, was observed for WT PB1 in influenza virus-infected cells (Fig. 1A and B, lanes WSN) and also reported by others (1, 4, 9). The biological significance of the second band remains unknown, but both bands were coprecipitated by the anti-PB2 antibody. Mutated PB1 proteins del 1 to del 7 formed stable complexes with PB2, as they were coimmunoprecipitated with PB2 by the anti-PB1 antibody. (Fig. 1A, PB2). Analysis of aliquots from the same lysates by using the anti-PB2 antibody also resulted in coprecipitation of PB2 along with mutated PB1 (Fig. 1B, lane del 1+PB2 to del 7+PB2), further confirming complex formation of the WT PB2 with mutant PB1 proteins. Again, both forms of PB1 were coprecipitated by the anti-PB2 antibody, indicating that both forms of the mutant PB1 formed complexes with PB2. However, the anti-PB2 antibody coprecipitated less PB1 in the immune complexes compared with the amount of PB2 coprecipitated by the anti-PB1 antibody. It is possible that the interaction of some anti-PB2 antibodies with PB2 protein may have destabilized some PB1-PB2 complexes and partially displaced some of the PB1 from the PB1-PB2 complex. Similar observation of differential immunoprecipitation of the components in the complex has been reported for Sendai virus P and L protein complexes, using coimmunoprecipitation methods (13, 26). Western immunoblotting data showed that the WT and mutant PB1 proteins were expressed at similar levels (data not shown).

Effect of large in-frame deletion of PB1 on complex formation with PB2. As individual deletion mutants (del 1 to del 7) spanning the entire PB1 sequence (except the first 33 aa) bound to PB2, there were two possibilities for the location of the PB2-binding site in PB1: either (i) PB2 bound to the first 33 aa or (ii) there were multiple PB2-binding sites in PB1 which

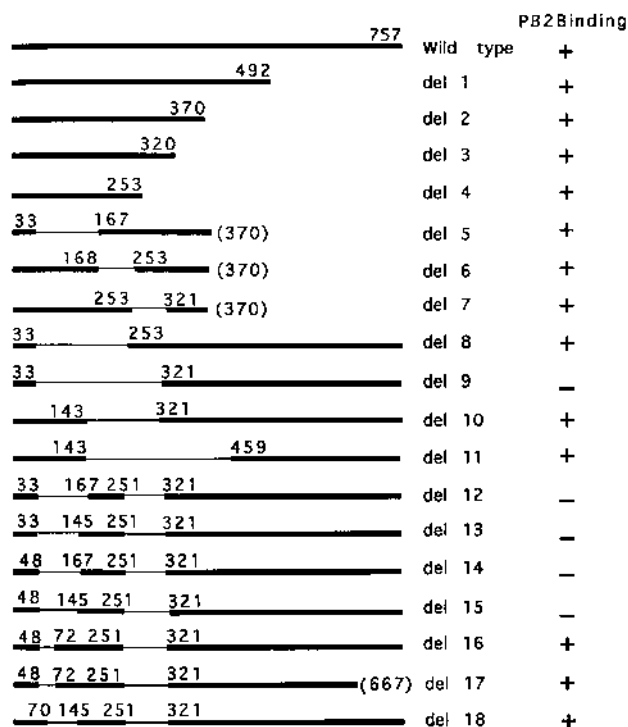


FIG. 2. Schematic representation of WT PB1 and deletion mutants. Thick line, PB1; thin line, in-frame deletion region; + and -, ability or inability of each PB1 mutant to form a stable complex with PB2. Numbers indicate positions of amino acids in the protein that are present in mutants del 1 to del 18.

TABLE 1. Polymerase activities of the deletion and linker-insertion mutants of PB1^a

| Mutant | Position of amino acid deleted or changed | New sequence ^b | % of WT CAT activity ^c |
|--------|---|---------------------------|-----------------------------------|
| WT | | | 100 |
| del 19 | 1–39 | /40MDTVNR45 | <0.1 |
| del 20 | 34–71 | 33G/72PLPED | <0.1 |
| del 21 | 71–121 | 71G/122LTQGR | <0.1 |
| del 22 | 49–144 | 48Q/S145NTIE | <0.1 |
| del 23 | 144–180 | 143L/V182TTHF | <0.1 |
| del 24 | 169–252 | 168K/253YFVE | <0.1 |
| L43 | 43 | 43VPLER44N | <0.1 |
| L168 | 168 | 167LNLEV168K | <0.1 |
| L252 | 252 | 252VSLEG253Y | <0.1 |
| L379 | 379 | 379KSARAD381F | <0.1 |
| L458 | 458 | 458GRSSG459I | <0.1 |
| L492 | 492 | 492FLEEF493T | <0.1 |
| L549 | 549 | 549QPLER550L | <0.1 |
| L667 | 667 | 667IPRGI668P | <0.1 |
| L746 | 746 | 746IPRGI747C | 85 |
| 443SA | 443 | 442QA444SDD | 82 |

^a All mutants bound PB2.^b Slashes represent deleted regions; new amino acids are underlined.^c Determined as reported previously (4).

could independently bind to PB2. To test the first possibility, 39 aa from the NH₂ terminus were deleted (del 19 [Table 1]), and del 19 was tested for PB2 binding by coexpression and coimmunoprecipitation. Results showed that deletion of the first 39 aa did not affect the PB2 binding activity (data not shown). To test the second possibility, four large in-frame deletion mutants of PB1 were constructed (Fig. 2, del 8 to del 11) and tested for the ability to form complexes with PB2 by coexpression with PB2 and coimmunoprecipitation. Results show that when the anti-PB1 antibody (Fig. 3A) was used, PB2 was coimmunoprecipitated as a complexes with del 8, del 10,

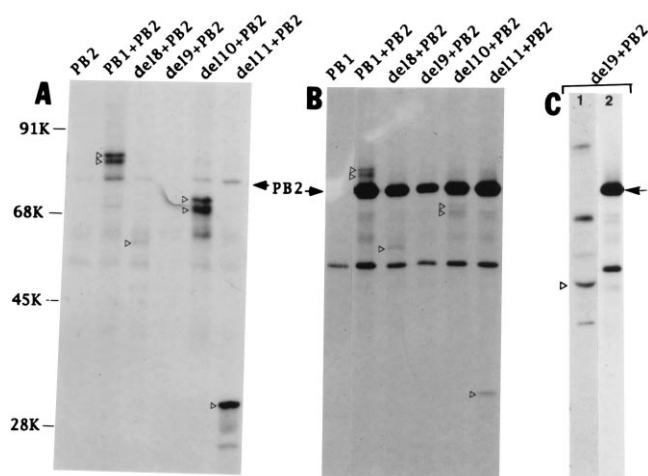


FIG. 3. Analysis of polymerase complex by coexpression of deleted PB1 (del 8 to del 11) and WT PB2. BHK-21 cells were infected with VTF7.3 at an MOI of 5 for 1 h and transfected either WT or mutated PB1 (del 8 to del 11) DNA along with WT PB2 DNA. The cells were labeled at 16 hpt and lysed. The cell lysate was divided into two parts, and each part was immunoprecipitated with a monospecific anti-PB1 (A and C, lane 1) or anti-PB2 (B and C, lane 2) antibody. Note that lane 1 in panel C had 10 times more anti-PB1 antibody. The polymerase complex was analyzed by SDS-PAGE. Positions of PB1 and PB2 are indicated as arrowheads and arrows. Note that a nonspecific band (~55 kDa) immunoprecipitated with the anti-PB2 antibody.

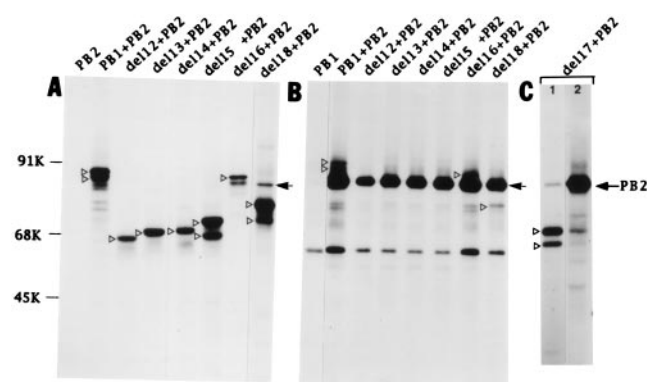


FIG. 4. Analysis of polymerase complex formation by coexpression of mutant PB1 (del 12 to del 18) and WT PB2. Cells were infected with VTF7.3 at an MOI of 5 for 1 h and then transfected with either WT PB1 or mutated PB1 (del 12 to del 18) along with WT PB2. The cells were labeled at 16 hpt and lysed. Aliquots were immunoprecipitated with either the anti-PB1 (A and C, lane 1) or anti-PB2 (B and C, lane 2) antibody. The immunoprecipitated polymerase complex was analyzed by SDS-PAGE. Positions of PB1 and PB2 are shown as arrowheads and arrows, respectively.

and del 11. Conversely, when the anti-PB2 antibody (Fig. 3B) was used for immunoprecipitations, PB2 was also found to form complexes with del 8, del 10, and del 11. On the other hand, del 9 protein was not precipitated by either the anti-PB1 or the anti-PB2 antibody. It should be also noted that when the anti-PB1 antibody was used, very little del 8 protein was immunoprecipitated (Fig. 3A, lane del8+PB2), possibly because the anti-PB1 antibody was raised against the first 377 aa of PB1 (2). Therefore, del 8 was only poorly recognized and del 9 was not recognized at all by the anti-PB1 antibody. However, when del 8 and del 9 were coexpressed with PB2, the anti-PB2 antibody immunoprecipitated the del 8 protein (Fig. 3B, del 8+PB2) but not the del 9 protein (Fig. 3B, lane del9+PB2). This lack of interaction of del 9 with PB2 could be explained in one of two ways: either del 9 was not expressed at all, or del 9 was expressed but did not interact with PB2. To test these possibilities, del 9 and PB2 were expressed together, and the product was divided into two parts; one part was immunoprecipitated with 10 times more anti-PB1 antibody (Fig. 3C, lane 1), and other part was immunoprecipitated with the normal amount of anti-PB2 antibody (Fig. 3C, lane 2). When 10 times more anti-PB1 antibody was used, a specific band of del 9 which did not bring down any PB2 was detected (Fig. 3C, lane 1, arrowhead). Note that a nonspecific band of 70,000 kDa (not PB2) was precipitated when 10 times more anti-PB1 antibody was used. Conversely, the anti-PB2 antibody did not coprecipitate del 9 PB1 (Fig. 3C, lane 2), indicating that PB2 did not interact with del 9 PB1. Again, a nonspecific protein of about 55,000 kDa was precipitated by the anti-PB2 antibody (Fig. 3B and C). These results led us to conclude tentatively that the PB1 region encompassing aa 34 through 320 contained the interacting sites for PB2.

Identification of the regions of PB1 protein important for binding to PB2. To determine definitively if the deletion of 287 aa in del 9 abolished the interaction with PB2 and to identify the specific domains present in this region responsible for PB2 binding, we constructed a series of in-frame double-deletion PB1 mutants (Fig. 2, del 12 to del 18). When double-deletion mutants were coexpressed with PB2, PB1 mutants del 11 to del 15 failed to bind any PB2 in assays using either the anti-PB1 (Fig. 4A) or anti-PB2 (Fig. 4B) antibody. del 15, which possesses a double deletion of 96 (residues 49 to 144) and 69

(residues 252 to 320) aa, contains the shortest deletion of PB1 which did not form any polymerase complex with PB2. To further define the region of 96 aa, two more double-deletion mutants (del 16 and del 18) were constructed. When del 16 and del 18 were expressed separately with PB2 and checked for complex formation, del 18 formed a complex with PB2 (Fig. 4A and B, lanes del18+PB2), but complex formation with del 16 could not be determined conclusively since the second band of del 16 and PB2 migrated in the same position in the gel (Fig. 4A and B, del16+PB2). Therefore, to determine if del 16 was interacting with PB2, 90 aa from the COOH terminus of del 16 were deleted to construct del 17. When del 17 was expressed together with PB2 and examined for complex formation with either the anti-PB1 (Fig. 4C, lane 1) or anti-PB2 (Fig. 4C, lane 2) antibody, the results showed that del 17 can bind with PB2 to form a complex. Since del 15 does not interact with PB2 but both del 16 (or del 17) and del 18 can form complexes with PB2, it appears that there are more than one binding site within the 96 amino acid residues (residues 49 to 144). Expression of individual polymerase proteins in transfected cells was assessed by Western immunoblotting and found to be similar for WT and mutant proteins. Taken together, these results show that there are multiple sites for PB2 interaction within the NH₂-terminal half of PB1 which can interact independently with PB2.

Interaction of PB1 mutants with WT PB2 in the presence of PA. The experiments described above were done in cells co-expressing PB1 and PB2 in the absence of PA, which is present in influenza virus-infected cells. To assess the biological significance of PB1-PB2 interaction in influenza virus replication, we examined the interaction of the WT and PB1 mutants with WT PB2 in the presence of PA. Accordingly, BHK-21 cells were infected with VTF7.3 and cotransfected with 4 μ g of PB1, 6 μ g of PB2, and 1.0 μ g of PA. A lower concentration of PA cDNA was used in these experiments, as the excess PA protein was found to cause proteolysis (32) and inhibition of polymerase activity (Fig. 5C). Cells were labeled at 16 hpt and immunoprecipitated separately by anti-PB1, anti-PB2, and anti-PA antibodies. Interactions of WT PB1 and PB1 mutants with PB2 were identical in the presence or absence of PA (data not shown). These results demonstrate that PB1 and PB2 interaction involving the same binding domains occurred in the presence or absence of PA and that PA does not interfere with PB1-PB2 interaction.

In vivo reconstitution of functional influenza virus transcription-replication complex by using ribozyme-mediated expression of synthetic influenza viral RNA. Earlier we developed an assay for influenza viruses polymerase in which individual components of the polymerase complex can be used to reconstitute the functional polymerase complex in vivo (4). In the present study, the assay system was further simplified by supplying all of the components, including template RNA through cDNA transfection. For this, a DNA template that directs the synthesis of synthetic template with precise 5' and 3' ends was constructed by accurate positioning of the 5' end to the T7 promoter site (18) and the 3' end before the cDNA sequence that encodes the self-cleaving ribozyme (3). To construct such a DNA template, we took advantage of plasmid IVACAT1 (18) and the Ribo-CAT transcription vector designated 2,0 (3). The construction of plasmid Ribo-CAT is described in Materials and Methods. When circular Ribo-CAT plasmid DNA was transcribed with T7 RNA polymerase, a discrete band corresponding to about 660 nucleotides was seen on the gel (data not shown), indicating that the ribozyme-mediated cleavage was essentially complete under the conditions of the transcription in vitro.

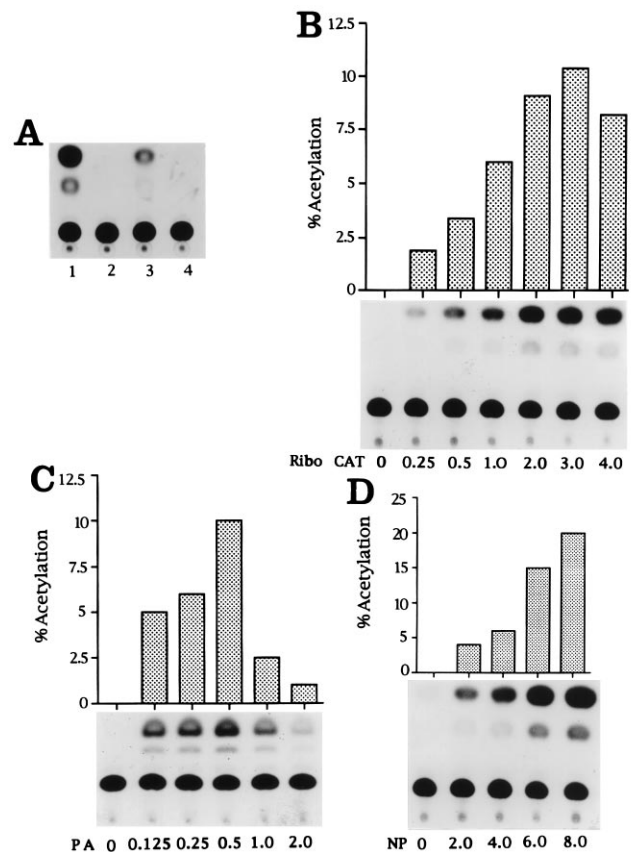


FIG. 5. Optimization of the influenza virus RNA transcription-replication assay using Ribo-CAT plasmid. COS1 cells in a 60-mm-diameter plate were infected with VTF7.3 at an MOI of 5 for 1 h and then transfected with PB1, PB2, PA, NP, and Ribo-CAT DNAs. Cells were incubated for 24 h, harvested, and assayed for CAT activity as described in Materials and Methods. (A) All cells were transfected with 4 μ g of NP, 2 μ g of PB2, and 0.5 μ g of PA DNA along with 1 μ g of Ribo-CAT DNA in lanes 1, 3, and 4, 1 μ g of pIVACAT1 (18) in lane 2, 2 μ g of PB1 DNA in lanes 1 and 2, and 0.5 μ g of PB1 DNA in lane 3. (B) Cells were transfected with PB1 (2 μ g), PB2 (2 μ g), PA (0.5 μ g), and NP (4 μ g) DNAs and various amounts of Ribo-CAT DNA. The numbers at the bottom indicate Ribo-CAT DNA amount in micrograms. (C) PB1 (2 μ g), PB2 (2 μ g), NP (4 μ g), and Ribo-CAT (2 μ g) DNAs and various amount of PA DNA. The numbers at the bottom represent micrograms of PA DNA. (D) Amounts of PB1 (2 μ g), PB2 (2 μ g), PA (0.5 μ g), and Ribo-CAT (3.0 μ g) DNAs remained constant and the amount (micrograms) of NP DNA was varied as shown at the bottom. Aliquots of cell lysates used for CAT assay were used for expression of polymerase proteins by Western immunoblotting. Expression levels were similar when same amounts of DNA were used for transfection in different experiments.

For the polymerase assay, COS1 cells were infected with VTF7.3 and subsequently transfected with a mixture of pGEM PB1, pGEM PB2, pGEM PA, pGEM NP, and Ribo-CAT DNAs. The efficiency of the transcription and replication of recombinant Ribo-CAT was measured by analyzing the CAT activity in the cell lysate at 24 hpt. Initial results demonstrated that CAT activity was present in transfected cells in which all influenza virus polymerase components were present (Fig. 5A, lanes 1 and 3). Omission of PB1 abolished the CAT activity (Fig. 5A, lane 4). In addition, omission of ribozyme and T7 termination sequence from Ribo-CAT abolished CAT activity (Fig. 5A, lane 3) even though these cells were transfected with pIVACAT1. These results demonstrated that ribozyme-mediated cleavage of RNA was essential to produce the precise 3' end of the synthetic viral RNA (Fig. 5A; compare lanes 1 and 2). Similarly, the omission of PB2 and NP also abolished CAT activity (data not shown).

To optimize the T7 transfection system for ribozyme-mediated CAT expression, we examined the quantitative relationship between the amount of CAT activity and the amount of transfected Ribo-CAT, pGEM PA, and pGEM NP DNAs. Accordingly, COS1 cells were infected with VTF7.3 at an MOI of 5 for 1 h and subsequently transfected with various amounts of Ribo-CAT DNA mixed with fixed amount of pGEM PB1, PB2, PA, and NP DNAs. The results showed that the CAT activity increased with increasing Ribo-CAT DNA concentration and reached its maximum at 3 μ g of Ribo-CAT DNA (Fig. 5B). However, further increasing the amount of Ribo-CAT DNA resulted in slightly decreasing CAT activity. When amounts of Ribo-CAT, pGEM PB1, pGEM PB2, and pGEM NP DNAs were kept constant and various amounts of pGEM PA DNA were used, CAT activity increased with increasing PA DNA concentration and reached a maximum at 0.5 μ g. However, a further increase of the pGEM PA DNA resulted in a dramatic decrease in CAT activity. The reduced CAT activity may be due to protease activity associated with PA protein (32). This might have resulted in decreasing the effective PB1, PB2, and NP protein concentrations in the cell, which in turn would produce less CAT protein. Interestingly, when the pGEM NP DNA concentration was increased while Ribo-CAT, pGEM PB1, pGEM PB2, and pGEM PA concentrations were kept constant, CAT activity increased with increasing NP concentration. A plateau was not reached even with 8 μ g of NP DNA. One explanation of the increased CAT activity may be that as the intracellular NP protein concentration increased, more Ribo-CAT RNA formed a CAT-RNP complex, which in turn was transcribed and replicated, causing an increased synthesis of CAT protein. Whether CAT activity could be increased further by adding more NP cDNA remains to be determined.

Polymerase activity of mutant PB1 proteins. The effects of the mutations introduced in the PB1 gene on its polymerase activity were studied by reconstitution of the active polymerase complex *in vivo*. The system described above, using Ribo-CAT DNA, is convenient and does not require transfection with either RNA or RNP complex (6, 16, 18–20). Using this Ribo-CAT system, we examined PB1 mutants for polymerase activity. In addition to PB1 deletion mutants, we also made in-frame linker insertions throughout the PB1 proteins. The amino acids generated by the linker insertions are shown in Table 1. The results of CAT activity obtained by thin-layer chromatography from two independent experiments are summarized in Table 1. None of the in-frame deletion mutations (Fig. 2) showed any CAT activity (data not shown). This was expected for mutants del 18 and del 19, which are deleted for portions of the PA-binding sequence (28), and del 23, which lacks the nuclear transport signal (23). However, since none of the other deletion mutants which were positive for PB2 binding showed any CAT activity, we suspected that structure perturbation of PB1 as a result of mutations caused the loss of polymerase activity. Therefore, we tested a series of linker insertions in PB1 for polymerase activity (12, 30). None of the linker-insertion mutants except L746 was positive in the CAT assay (Table 1), although all of them were positive in a PB2 binding assay (data not shown). L-746 was near the COOH-terminal region of PB1. Point mutation 443SA, (serine at position 443 of the polymerase domain changed to alanine) exhibited CAT activity in this assay. This finding is in good agreement with our previous results (4). Thus, it appears that polymerase activity was highly sensitive to deletion or linker-insertion mutation of PB1 irrespective of the ability to form a complex with PB2.

DISCUSSION

Interactions among the influenza virus polymerase proteins (PB1, PB2, and PA) are important for transcription and replication of viral RNA (4, 15, 17). The goal of the experiments reported here was to identify the regions of PB1 responsible for binding to PB2 by using the VTF7.3-derived cDNA expression system. The interaction of PB1 and PB2 was not disrupted by deletion of two-thirds of the COOH-terminal region of PB1. As shown in Fig. 3 and 4, there are two or more binding sites spanning 96 (aa 49 to 144) and 69 (aa 252 to 320) aa within the NH₂-terminal region of PB1. Each binding site can bind to PB2 independently of the other. Deletion analysis of 97 aa indicates that there could be more than one binding site within this region, since both del 16-del 17 and del 18 can bind to PB2 independently. One interesting feature regarding the position of the PB2-binding sites is that one is located at the NH₂ terminus and the other is at the COOH terminus of the bipartite nuclear localization signal (23). It will therefore be possible to examine whether complex formation occurs predominantly in the nucleus after components of the polymerase complex enter the nucleus individually or complex formation occurs in the cytoplasm before nuclear entry and the polymerase enters the nucleus as a complex. Also, the first PB2-binding site (aa 49 to 144) is located immediately after the first 48 aa containing the PA-binding region (28). From comparison of the PB1 protein sequences of different types of influenza viruses, it appears that the two most conserved regions between aa 120 to 146 and aa 250 to 312 of PB1 are located within the PB2-binding sites (36). Moreover, the 69-aa binding site spanning aa 252 to 320 of PB1 overlaps polymerase motif I (4, 29). The binding PB2 to motif I may aid PB2 in positioning the cleaved cap structure to the close proximity of the active polymerase module. Further, secondary structure analysis (33) indicates that the second binding site, spanning aa 252 to 320, represents an α helix surrounded by β -plated sheet and β turn at its NH₂ and COOH termini, respectively. The first binding site represents α helix followed by β -plated sheets. There are three cysteine residues in the NH₂-terminal half of PB1, and these are within these two PB2-binding sites. It will be interesting to examine whether the cysteine residues play any role in disulfide bond formation, thereby bringing the two binding sites together.

There was a quantitative difference among the different PB1 mutants in the ability to form a complex with PB2. Although quantitative differences may shed further light in the nature of complex formation, it is difficult to assess the significance of these quantitative differences in our experiments for a number of reasons. (i) Polyclonal antibodies were prepared against specific regions of denatured proteins (1). Therefore, these antibodies may react differently to different mutant proteins which may have undergone conformational changes as a result of deletion. (ii) Some antibodies may bind to portions of the interacting regions and thus may react inefficiently to the complex or may destabilize or even displace the heterologous protein from weak complexes. This could explain why the anti-PB2 antibody coprecipitated less PB1 compared with the amount of PB2 immunoprecipitated by the anti-PB1 antibody in the complex. It is therefore possible that there are other interacting regions which we have not detected. Obviously, the affinities and strengths of the interacting domains of PB1 and PB2 need to be examined in detail, using finer deletions and site-specific mutations of individual amino acids. Such experiments are under way.

In this report, we have also described an *in vivo* influenza virus polymerase assay simplified by omitting the RNA or RNP transfection step (4, 7, 16, 18, 20). In this system, all compo-

nents including the Ribo-CAT template under the control of the T7 promoter were introduced by transfection in VTF7.3-infected cells. Similar assay systems have been recently reported by others (28a, 37). The data presented in this paper show that the polymerase assay (CAT activity) was consistently reproducible and that critical concentrations of PA and NP cDNAs are required for optimal polymerase activity. A similar requirement of PA has been reported by others (20, 32). Using this system, we have analyzed the effects of mutations in PB1 on influenza virus transcriptase/replicase activity. Data presented here showed that any in-frame deletion mutation of PB1 makes the polymerase protein inactive although the mutants formed complexes with PB2. Also, most of the linker-insertion mutations which also formed complexes with PB2 were also inactive; the exception was the construct with a mutation in the COOH-terminal end. Previously, we have shown that PB1 possesses four conserved structural motifs required for polymerase activity (4). Studies reported here show that in addition to the four critical motifs, the proper structure of PB1 is also critical for its biological activity. Similar results for the structural requirement of PB2 were obtained by Perales et al. (27), who observed that the polymerase activity was abolished when PB2 was mutated by single amino acid insertion or in-frame deletions.

In conclusion, we have shown that multiple sites of PB1 can interact independently with PB2, and this finding will enable us to define the corresponding PB2-binding sites for each PB1-binding region. Furthermore, we have also presented a simplified assay for reconstituting the active influenza virus polymerase complex *in vivo*; using this assay, we found that PB1 is highly sensitive to structural perturbation for polymerase activity.

ACKNOWLEDGMENTS

Work reported here was partially supported by NIAID/NIH grants AI-12749 and AI-16348.

We thank Eleanor Berlin for typing the manuscript.

REFERENCES

- Akkina, K. R., J. C. Richardson, M. C. Aguilera, and C. M. Yang. 1991. Heterogeneous form of polymerase proteins exist in influenza A virus-infected cells. *Virus Res.* **19**:17–30.
- Akkina, R. K., T. M. Chambers, D. R. Londo, and D. P. Nayak. 1987. Intracellular localization of the viral polymerase proteins in cells infected with influenza virus and cells expressing PB1 protein from cloned cDNA. *J. Virol.* **61**:2217–2224.
- Ball, L. A. 1992. Cellular expression of a functional nodavirus RNA replicon from vaccinia virus vectors. *J. Virol.* **66**:2335–2345.
- Biswas, S. K., and D. P. Nayak. 1994. Mutational analysis of the conserved motifs of influenza A virus polymerase basic protein 1. *J. Virol.* **68**:1819–1826.
- Cianci, C., L. Tiley, and M. Krystal. 1995. Differential activation of the influenza virus polymerase via template RNA binding. *J. Virol.* **69**:3995–3999.
- de la Luna, S., J. Martin, A. Portela, and J. Ortin. 1993. Influenza virus naked RNA can be expressed upon transfection into cells co-expressing the three subunits of the polymerase and the nucleoprotein from SV 40 recombinant viruses. *J. Gen. Virol.* **74**:535–539.
- Detjen, B. M., C. St. Angelo, M. G. Katze, and R. M. Krug. 1987. The three influenza virus polymerase (P) proteins not associated with viral nucleocapsids in the infected cell are in the form of a complex. *J. Virol.* **61**:16–22.
- Fodor, E., D. C. Pritlove, and G. G. Brownlee. 1994. The influenza virus panhandle is involved in the initiation of transcription. *J. Virol.* **68**:4092–4096.
- Fodor, E., B. L. Seong, and G. G. Brownlee. 1993. Photochemical cross-linking of influenza A polymerase to its virion RNA promoter defines a polymerase binding site at residues 9 to 12 of the promoter. *J. Gen. Virol.* **74**:1327–1333.
- Fuerst, T. R., A. L. Earl, and B. Moss. 1987. Use of a hybrid vaccinia virus-T7 RNA polymerase system for expression of target genes. *Mol. Cell. Biol.* **7**:2538–2544.
- Hagen, M., T. D. Y. Chung, J. A. Butcher, and M. Krystal. 1994. Recombinant influenza virus polymerase: requirement of both 5' and 3' viral ends for endonuclease activity. *J. Virol.* **68**:1509–1515.
- Hizi, A., A. Barber, and S. H. Huges. 1989. Effects of small insertions on the RNA-dependent DNA polymerase activity of HIV-1 reverse transcriptase. *Virology* **170**:326–329.
- Horikami, S. M., J. Curran, D. Kolakofsky, and S. A. Moyer. 1992. Complexes of Sendai virus NP-P and P-L proteins are required for defective interfering particle genome replication *in vitro*. *J. Virol.* **66**:4901–4908.
- Hsu, M., J. D. Parvin, S. Gupta, M. Krystal, and P. Palese. 1987. Genomic RNAs of influenza viruses are held in a circular conformation in virions and in infected cells by a terminal panhandle. *Proc. Natl. Acad. Sci. USA* **84**:8140–8144.
- Huang, T.-S., P. Palese, and M. Krystal. 1990. Determination of influenza virus proteins required for genome replication. *J. Virol.* **64**:5669–5673.
- Kimura, N., M. Nishida, K. Nagata, A. Ishihama, K. Oda, and S. Nakada. 1992. Transcription of a recombinant influenza virus RNA in cells that can express the influenza virus RNA polymerase and nucleoprotein genes. *J. Gen. Virol.* **73**:1321–1328.
- Krug, R. M., F. V. Alosio-Caplen, I. Julkunen, and M. G. Katze. 1989. Expression and replication of the influenza virus genome, 89–152. *In* R. M. Krug (ed.), *The influenza viruses*. Plenum Press, New York.
- Luytjes, W., M. Krystal, M. Enami, J. D. Parvin, and P. Palese. 1989. Amplification, expression and packaging of a foreign gene by influenza virus. *Cell* **59**:1107–1113.
- Mena, I., S. de la Luna, C. Albo, J. Martin, A. Nieto, J. Ortin, and A. Portela. 1994. Synthesis of biologically active influenza virus core proteins using a vaccinia-T7 RNA polymerase expression system. *J. Gen. Virol.* **75**:2109–2114.
- Mena, I., S. de la Luna, J. Martin, C. Albo, B. Perales, A. Nieto, A. Portela, and J. Ortin. 1995. Systems to express recombinant RNA molecules by the influenza A virus polymerase *in vivo*, p. 329–342. *In* K. W. Adolph (ed.), *Methods in molecular genetics, Molecular virology techniques*, part B. Academic Press, Inc., Orlando, Fla.
- Mukaigawa, J., and D. P. Nayak. 1991. Two signals mediate nuclear localization of influenza virus (A/WSN/33) polymerase basic protein 2. *J. Virol.* **65**:245–253.
- Nakagawa, Y., N. Kimura, T. Toyoda, K. Mizumoto, A. Ishihama, K. Oda, and S. Nakada. 1995. The RNA polymerase PB2 subunits is not required for replication of the influenza virus genome but is involved in capped mRNA synthesis. *J. Virol.* **69**:728–733.
- Nath, S. T., and D. P. Nayak. 1990. Function of two discrete regions is required for nuclear localization of polymerase basic protein 1 of A/WSN/33 influenza virus (H1 N1). *Mol. Cell. Biol.* **10**:4139–4145.
- Neumann, G., A. Zobel, and G. Hobom. 1994. RNA polymerase I-mediated expression of influenza viral RNA molecules. *Virology* **202**:477–479.
- Nieto, A., S. de la Luna, J. Barcena, A. Portela, J. Valcarcel, J. A. Melero, and J. Ortin. 1992. Nuclear transport of influenza virus polymerase PA protein. *Virus Res.* **24**:65–75.
- Parks, G. D. 1994. Mapping of a region of the paramyxovirus L protein required for the formation of a stable complex with the viral phosphoprotein P. *J. Virol.* **68**:4862–4872.
- Perales, B., S. de la Luna, I. Palacios, and J. Ortin. 1996. Mutational analysis identifies functional domains in the influenza A virus PB2 polymerase subunit. *J. Virol.* **70**:1678–1686.
- Perez, D. R., and R. O. Donis. 1995. A 48-amino-acid region of influenza A virus PB1 protein is sufficient for complex formation with PA. *J. Virol.* **69**:6932–6939.
- 28a. Pleschka, S., S. R. Jaskunas, O. G. Engelhardt, T. Zurcher, P. Palese, and A. Garcia-Sastre. 1996. Plasmid-based reverse genetics system for influenza A virus. *J. Virol.* **70**:4188–4192.
- Poch, O., I. Sauvaget, M. Delarue, and N. Tordo. 1989. Identification of four conserved motifs among the RNA-dependent polymerase encoding elements. *EMBO J.* **8**:3867–3874.
- Prasad, V. R., and S. P. Goff. 1989. Linker-insertion mutagenesis of the human immunodeficiency virus reverse transcriptase expressed in bacteria: definition of the minimal polymerase domain. *Proc. Natl. Acad. Sci. USA* **86**:3104–3108.
- Sambrook, J., E. F. Fritsch, and T. Maniatis. 1989. *Molecular cloning of laboratory mammal*, 2nd ed. Cold Spring Harbor Laboratory Press, Cold Spring Harbor, N.Y.
- Sanz-Ezquerro, J. J., S. de la Luna, J. Ortin, and A. Nieto. 1995. Individual expression of influenza virus PA protein induces degradation of expression proteins. *J. Virol.* **69**:2420–2426.
- Sivasubramanian, N., and D. P. Nayak. 1982. Sequence analysis of the polymerase 1 gene and secondary structure prediction of polymerase 1 protein of human influenza virus A/WSN/33. *J. Virol.* **44**:321–329.
- St. Angelo, C., G. E. Smith, M. D. Summers, and R. M. Krug. 1987. Two of the three influenza viral polymerase proteins expressed by using baculovirus vectors form a complex in insect cells. *J. Virol.* **61**:361–365.
- Tiley, L. S., M. Hagen, J. T. Matthews, and M. Krystal. 1994. Sequence specific binding of the influenza virus RNA polymerase to sequences located at the 5' ends of the viral RNAs. *J. Virol.* **68**:5108–5116.
- Yamashita, M., M. Krystal, and P. Palese. 1989. Comparison of the three large polymerase proteins of influenza A, B, and C viruses. *Virology* **171**:458–466.
- Zhang, H., and G. M. Air. 1994. Expression of functional influenza virus polymerase proteins and template cloned from cDNAs in recombinant vaccinia virus-infected cells. *Biochem. Biophys. Res. Commun.* **200**:95–101.